Supporting Information

Development of a Modular NTA:His Tag Viral Vaccine for Co-delivery of Antigen and Adjuvant

Young Hun Chung[1,2], Britney A. Volckaert[3], Nicole F. Steinmetz[1,2,3,4,5,6,7*]

[1]Department of Bioengineering, University of California, San Diego, La Jolla, CA, 92093, United States
[2]Moores Cancer Center, University of California, San Diego, La Jolla, CA, 92093, United States
[3]Department of NanoEngineering, University of California, San Diego, La Jolla, CA, 92093, United States
[4]Department of Radiology, University of California, San Diego, La Jolla, CA, 92093, United States
[5]Institute for Materials Discovery and Design, University of California, San Diego, La Jolla, CA, 92093, United States
[6]Center for Nano-ImmunoEngineering, University of California, San Diego, La Jolla, CA, 92093, United States
[7]Center for Engineering in Cancer, Institute for Engineering in Medicine, University of California, San Diego, La Jolla, CA, 92093, United States

*corresponding author: nsteinmetz@ucsd.edu

Figure S1. Dithiothreitol (DTT) reduction of CPMV-NiNTA and binding intermediaries. Nickel (Ni), in the presence of DTT, becomes reduced causing a change in color of the solution to brown. While CPMV and CPMV-NTA (no Ni) stay clear, the CPMV-NiNTA solution turns brown indicating that after purification, Ni remains within the solution bound to the CPMV-NTA.

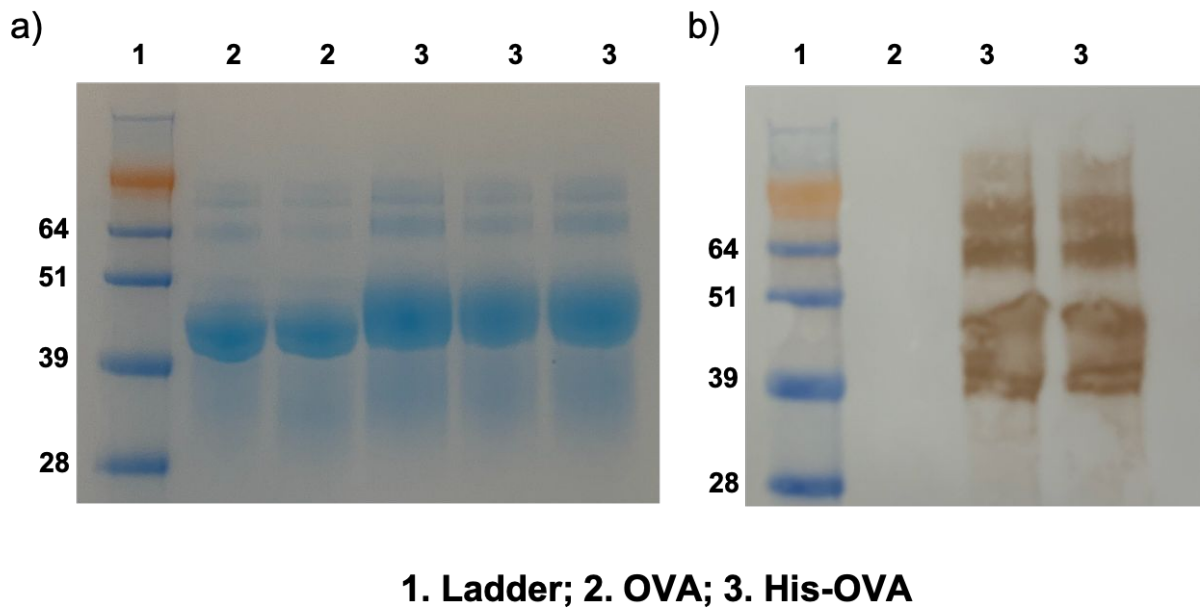

Figure S2. SDS-PAGE and WB of His-OVA. a) SDS-PAGE. Following His-tagging of OVA, the molecular weight of the OVA increases slightly resulting in slower electrophoretic mobility. b) WB against the His-tag. The WB indicates that the His moiety is conjugated to OVA with no background in the native OVA sample.

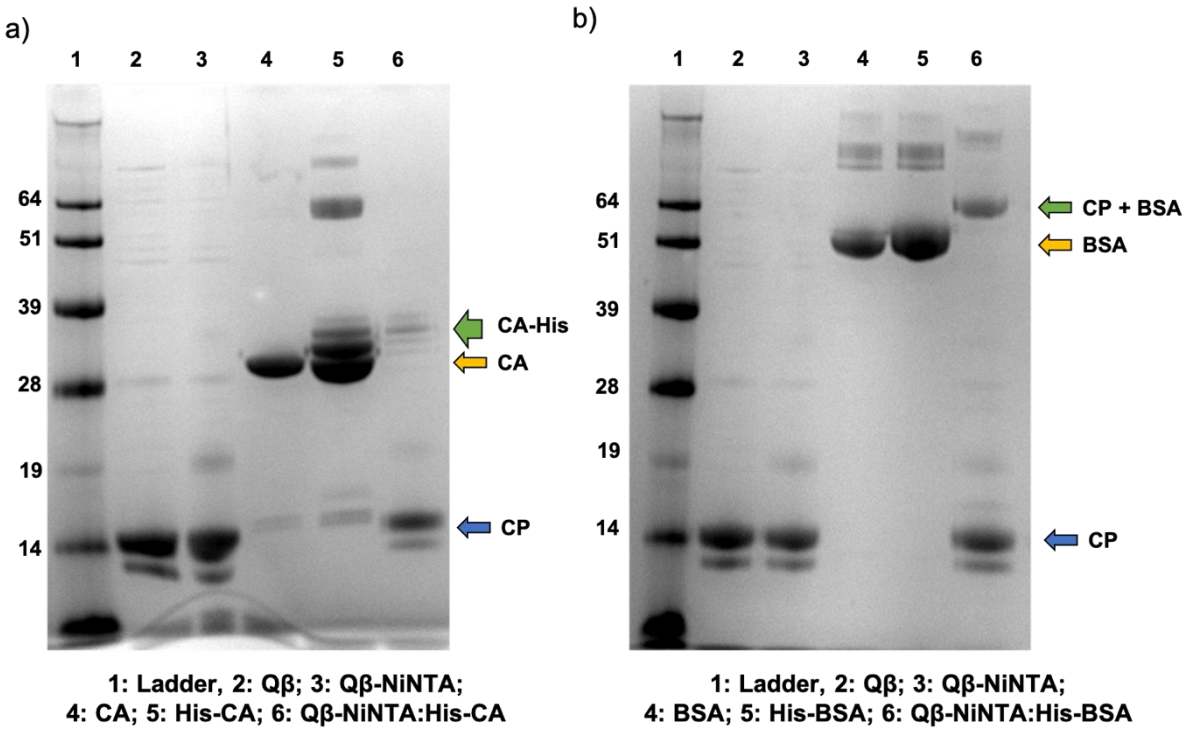

Figure S3. Demonstration of plug-and-play capabilities of the CPMV/Qβ-NiNTA formulations. a) SDS-PAGE of Qβ-NiNTA:His-carbonic anhydrase (CA). For Qβ-NiNTA:His-CA, only His-tagged CA is detectable indicating free CA is removed during purification. b) SDS-PAGE of the Qβ-NiNTA:His-BSA. A characteristic upwards shift of the protein band indicates binding of the CP to BSA (as was observed for OVA, see Figure 2).

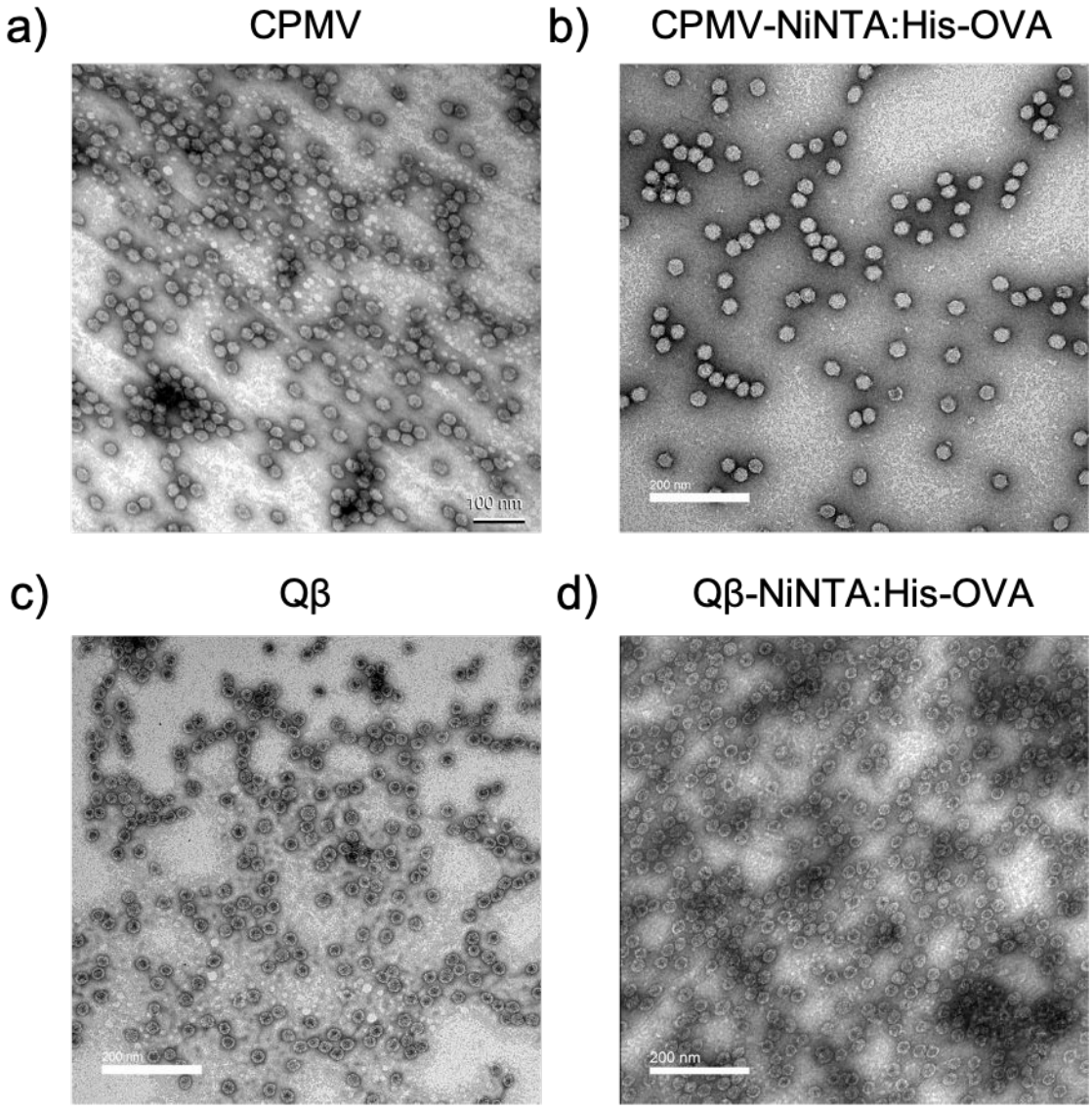

Figure S4: TEM of native and OVA-bound virus particles. TEM of a) CPMV, b) CPMV-NiNTA:His-OVA, c) Qβ, and d) Qβ-NiNTA:His-OVA. The scale bar in a) is 100 nm while the scale bars in b) are at 200 nm.

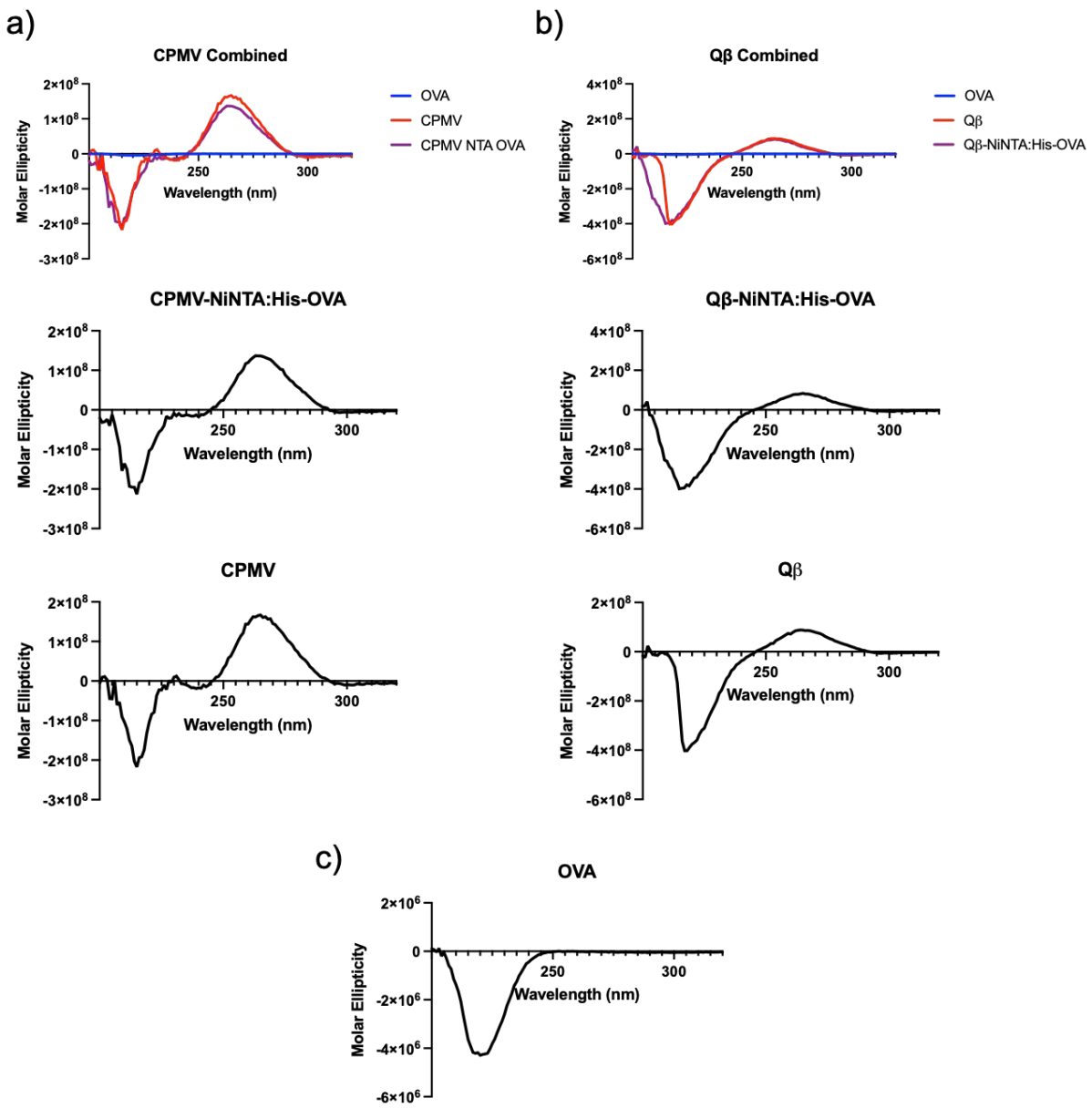

Figure S5: Circular dichroism spectra of native and OVA-bound virus nanoparticles. Spectra of a) CPMV-NiNTA:His-OVA, CPMV, and the overlayed graphs, b) Qβ, Qβ-NiNTA:His-OVA, and the overlayed graphs, and c) OVA. The overlayed CPMV/Qβ and the OVA-bound CPMV/Qβ spectra show minimal changes indicating that the binding of OVA does not influence the secondary/tertiary structure of the virus.

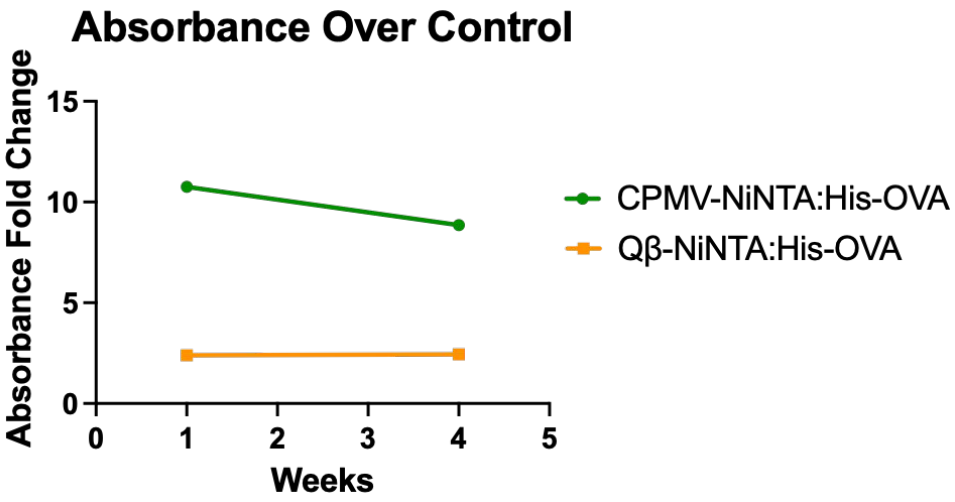

Figure S6: Longitudinal analysis of OVA binding with ELISAs. The absorbance values of the CPMV/Qβ-NiNTA:His-OVA were compared to the absorbance of CPMV/Qβ, respectively, with respect to time. The ELISAs demonstrate that even up to 4 weeks past the generation of the vaccines, they are still able to bind OVA leading to significantly greater signal compared to controls.

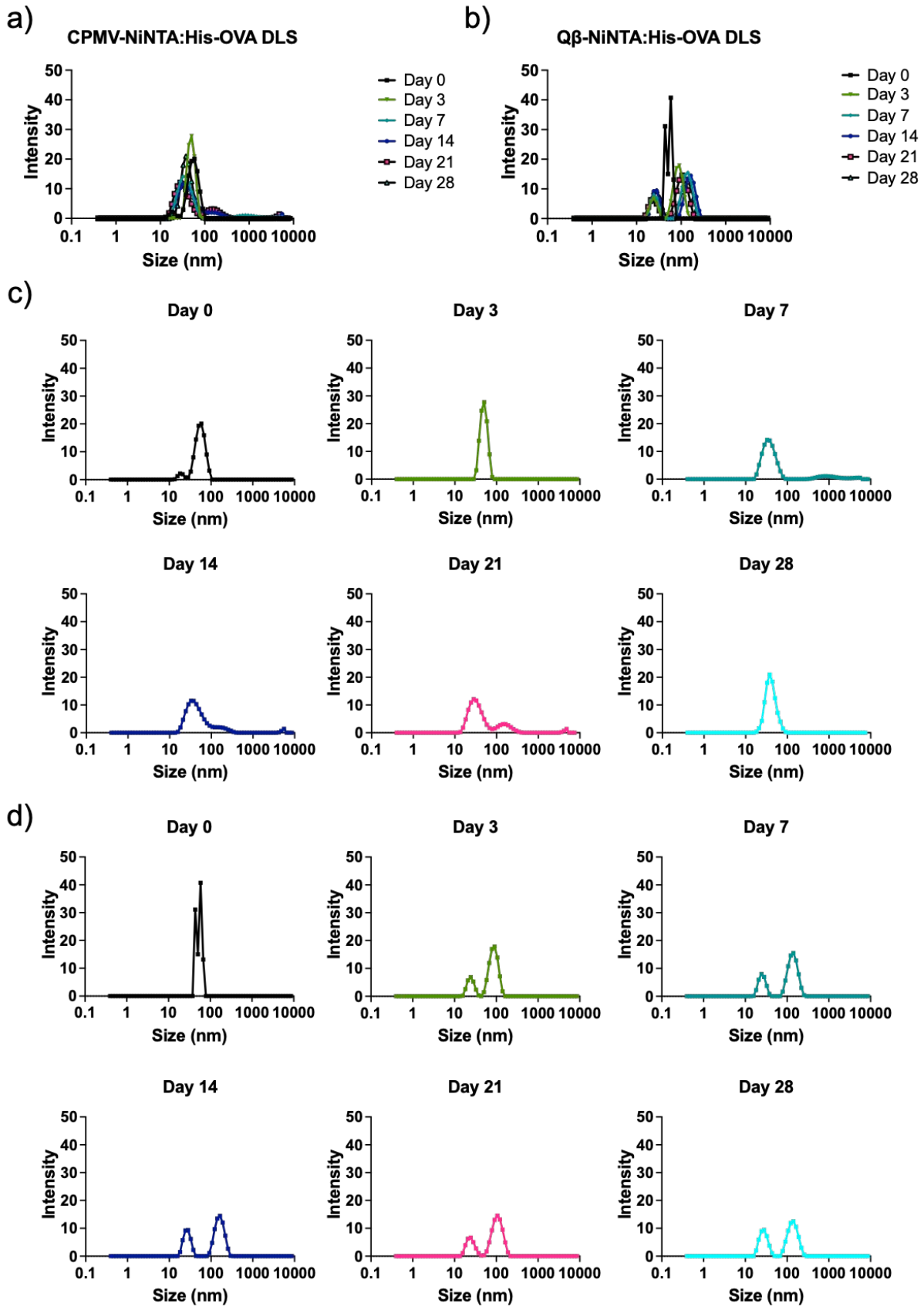

Figure S7: Longitudinal analysis of CPMV/Qβ-NiNTA:His-OVA by DLS. a) Overlayed DLS spectra of CPMV-NiNTA:His-OVA. b) Overlayed DLS spectra of Qβ-NiNTA:His-OVA. c) CPMV-NiNTA:His-OVA DLS spectra as a function of time. d) Qβ-NiTNA:His-OVA DLS spectra as a function of time.

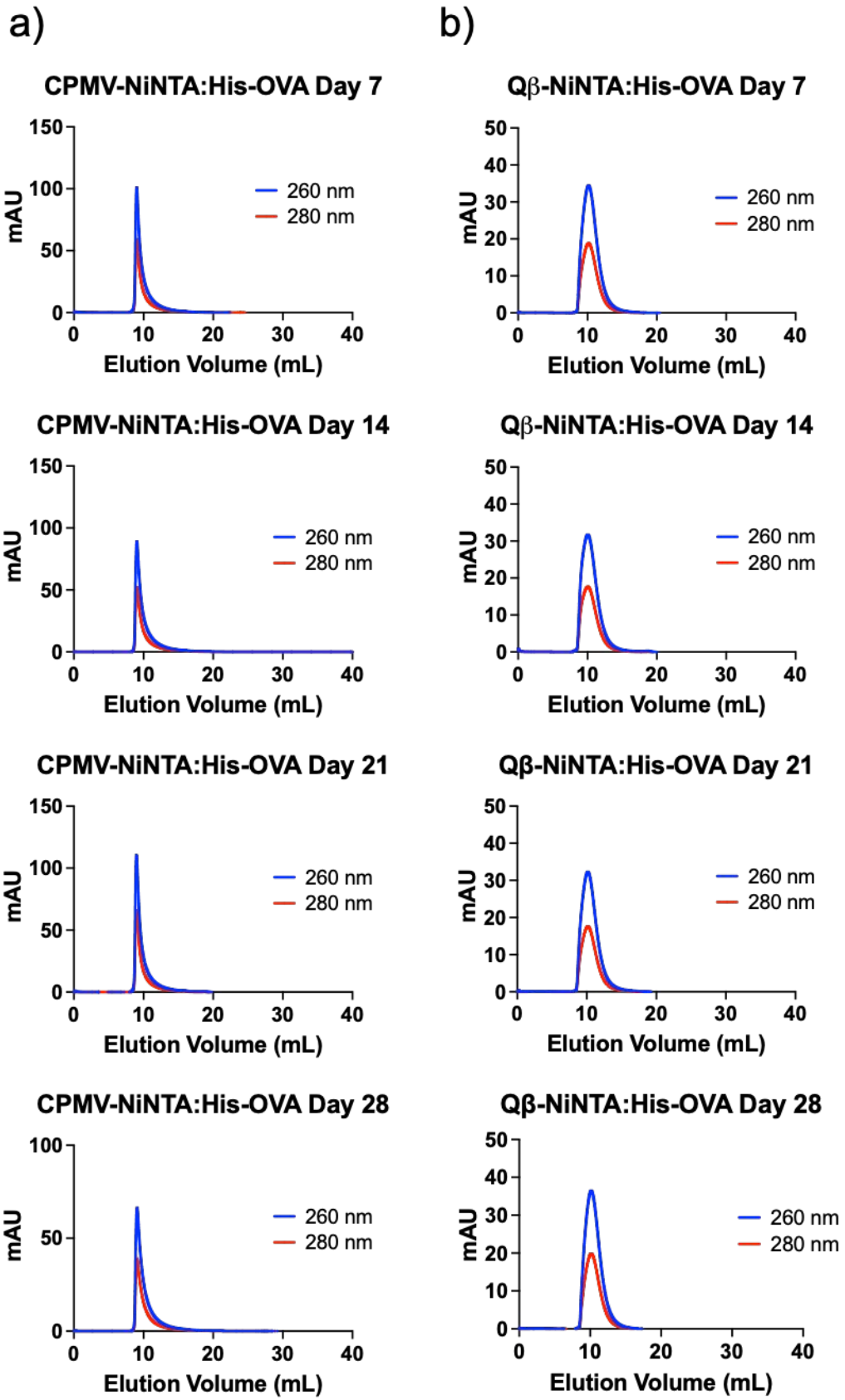

Figure S8: Longitudinal analysis of CPMV/Qβ-NiNTA:His-OVA by FPLC. a) FPLC graphs of CPMV-NiNTA:His-OVA as a function of time. b) FPLC graphs of Qβ-NiNTA:His-OVA as a function of time.

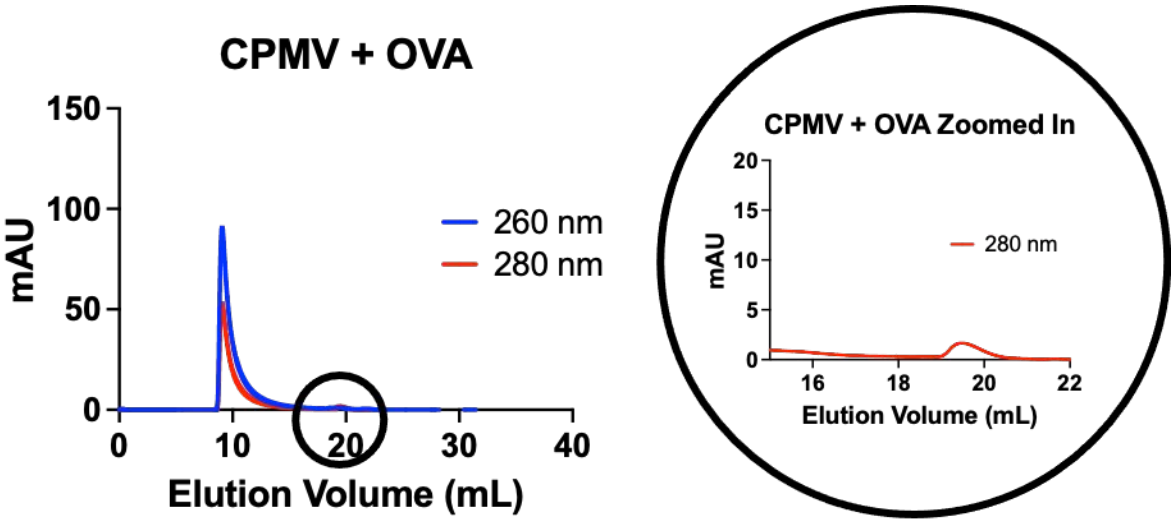

Figure S9: FPLC of native CPMV with unbound OVA. The OVA concentration injected was determined based upon the number of OVA bound per CPMV. At around 20 mL elution volume, there is a small absorbance peak at the 280 nm wavelength indicating the elution of the free OVA.

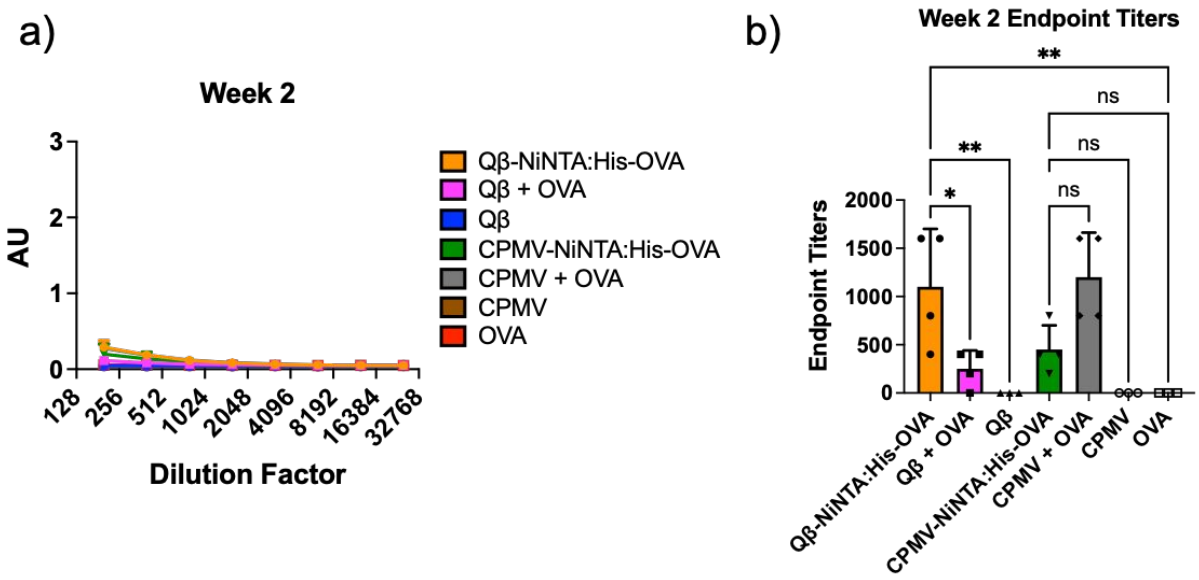

Figure S10. Week 2 antibody production. a) ELISA of the week 2 antibody production. b) Endpoint titers of samples from a). The endpoint titer was determined as the dilution at which the absorbance was twice that of the blank. * = $p < 0.05$, ** = $p < 0.01$, ns = not significant. The endpoint titers were analyzed using one-way ANOVA, and all analyses were done on GraphPad Prism.

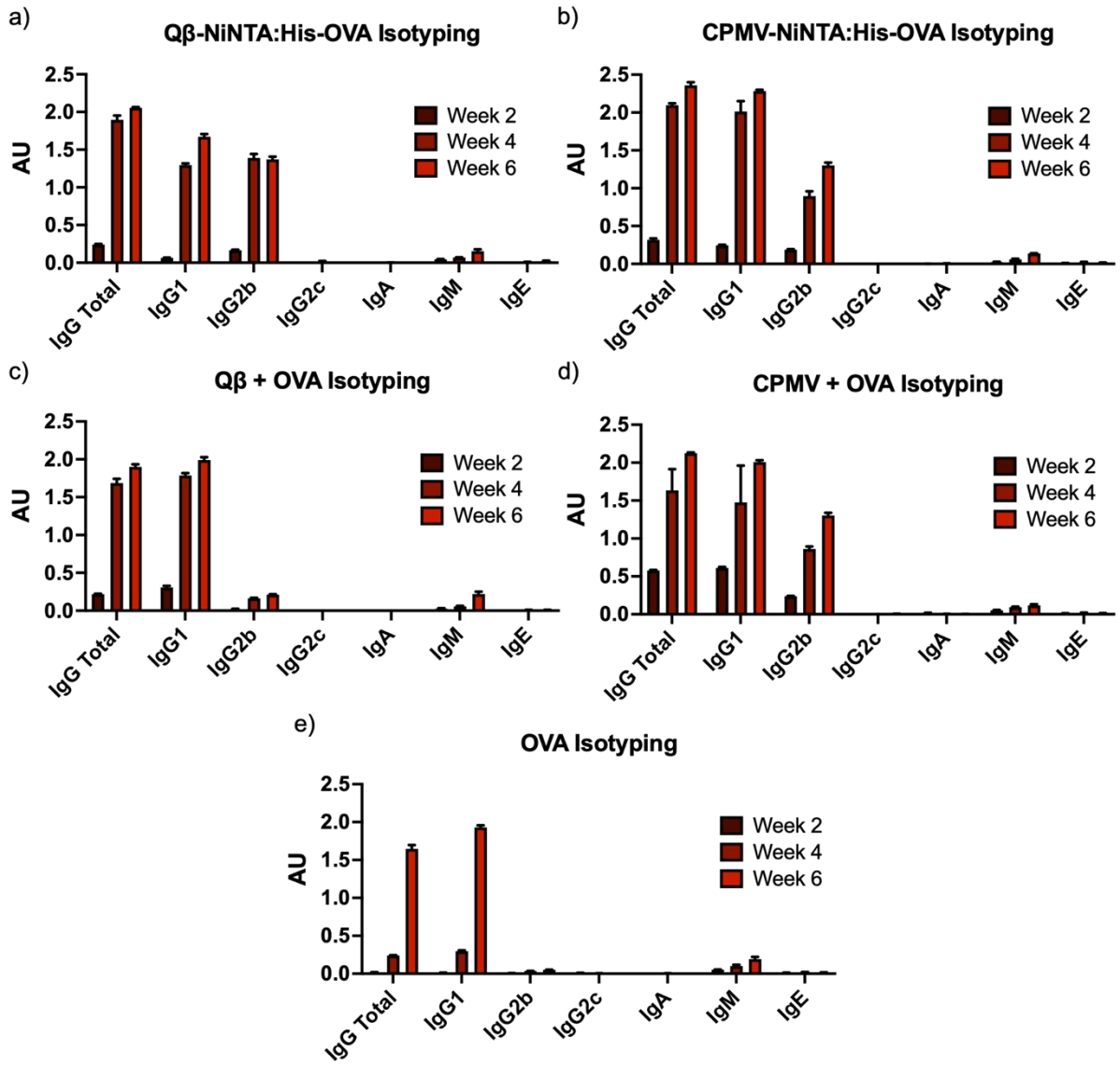

Figure S11. Full antibody isotyping. Isotyping was accomplished on the antibodies from weeks 2 – 6 for a) Qβ-NiNTA:His-OVA, b) CPMV-NiNTA:His-OVA, c) Qβ + OVA, d) CPMV + OVA, and e) OVA.

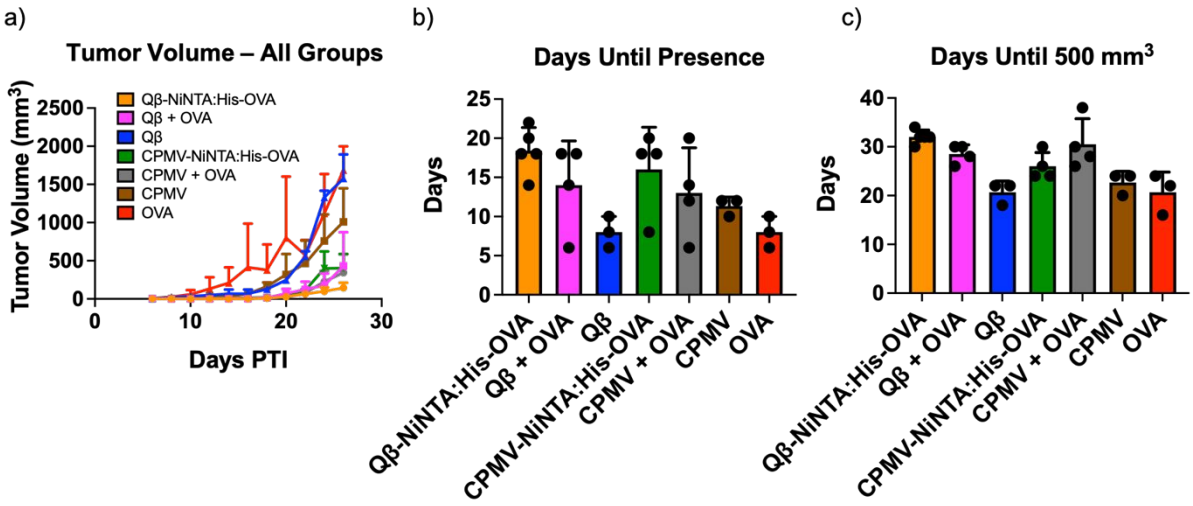

Figure S12. Tumor volume curve and delayed onset of tumor development graphs of all groups. a) Tumor volume curve of all groups. b) Average number of days until the tumors were palpable. c) Average number of days until the tumors reached 500 mm^3. Tumor volumes were measured using the equation: $V = l \times w^2/2$.

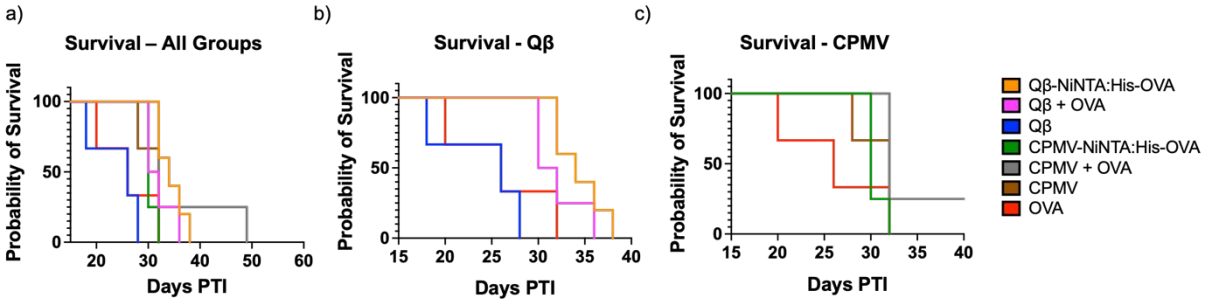

Figure S13. Survival curves of the mice in Figure 4. The survival curves are shown for a) all groups, b) only the Qβ groups, and c) only the CPMV groups. The b,c) curves were separated for ease of viewing.